

# STUDY OF STRUCTURE AND PHYSICO-CHEMICAL AND MECHANICAL PROPERTIES IN LOW-CARBON STEEL AFTER CYCLIC LOADING

L.A. Gorbachyov\*, A.D. Pogrebnjak\*\*

\*East Kazakhstan State Technical University (Ust-Kamenogorsk)  
Kazakhstan

\*\*Sumy Institute for Surface Modification  
Ukraine

Received 26.02.2009

It has been determined by Auger-analysis method, roentgenofluorescence method, and the diffraction analysis that dark spots which appear in the examined steel under cyclic loading are new phases.

Dark spots appear in the microstructures of some balanced condition metals (carbon steels, copper, polycrystals of lead [1] and others) when they are exposed to cyclic loading. At the initial stage, they appear as separate small darkenings, which can further spread over all metal grains and cover a considerable part of the deformed area, especially when it is close to metal failure.

Fig. 1 shows the temperature kinetic fatigue curve with the points of observation and the microstructure corresponding to these points; dashed lines and Roman figures show the division into failure time stages.

In our paper [2] we suggested distinguishing the following stages of the fatigue failure process:

1. Incubatory stage.
2. The stage of slip bands active formation.
3. The stage of local accumulation of damage and changes which occurred during the first and the second phases.
4. The main crack propagation and growth stage.
5. The sample failure stage. The duration of this stage for light section samples is insignificant.

As it can be seen in fig. 1, when the stage of slip bands active formation is over (point of observation 2), no new slip bands appear, but the dark spots prominence and density gradually increase and peak at the end of the third stage (point of observation 3). This fact can indicate the final depletion of the sample ductility reserve in the deformed area and its transition to a brittle failure stage.

A lot of research of this phenomenon has been done, for example [3], but the causes and the nature of these spots are not clear yet.

Earlier in [4] we suggested a presumable interpretation of these spots appearance and propagation causes.

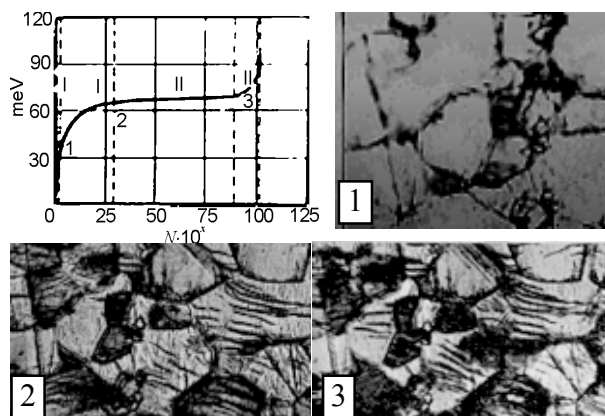


Fig. 1. The kinetic fatigue curve and the photos of microstructures corresponding to observation points 1, 2, 3 on the curve.

First, these are the “weakest” grains and their areas. Under the unfavourable conditions of a flow shear they experience the primary impact of high cyclic loading of the same sign – compression – which causes their active cyclic deformation. These spots prominence can indicate pressing out considerable amounts of metal.

Second, the active repeated cyclic compression strain in these amounts of metal causes their intensive heating which promotes these microscopic volumes active oxidation. This process can have a complex and specific nature due to the cycling of loading and its frequency.

These spots are likely to have the same nature as the aeration along the slip bands. They intensively appear on rimmed steel which features high ductility and gas content. Therefore, the intensity of these spots can be related to the gas content of the material itself. The more so, as these spots appear when similar materials are tested in vacuum [5].

In this paper we analyze the microstructure of lamellar samples of low-carbon steel of the content  $C = 0.05 - 0.12\%$ ;  $Mn = 0.25 - 50\%$ ;

Si = 0.03% of 1×10 mm effective section under the cyclic loading of alternating bending with the frequency of cycling equal to 2800 cycle per minute at the installation with the permanent total amplitude [6].

## SURFACE ALTERATIONS EXAMINATION

To analyse the profile we got a 3-D image of the sample's initial and cyclically deformed areas surfaces. Fig. 2 shows the profilograms of the sample's initial area (left) and its deformed area (right).

Fig. 2 shows how significant the surface alterations are under the cyclic loading. A special attention should be given to the amount of the deformed metal pressing out.

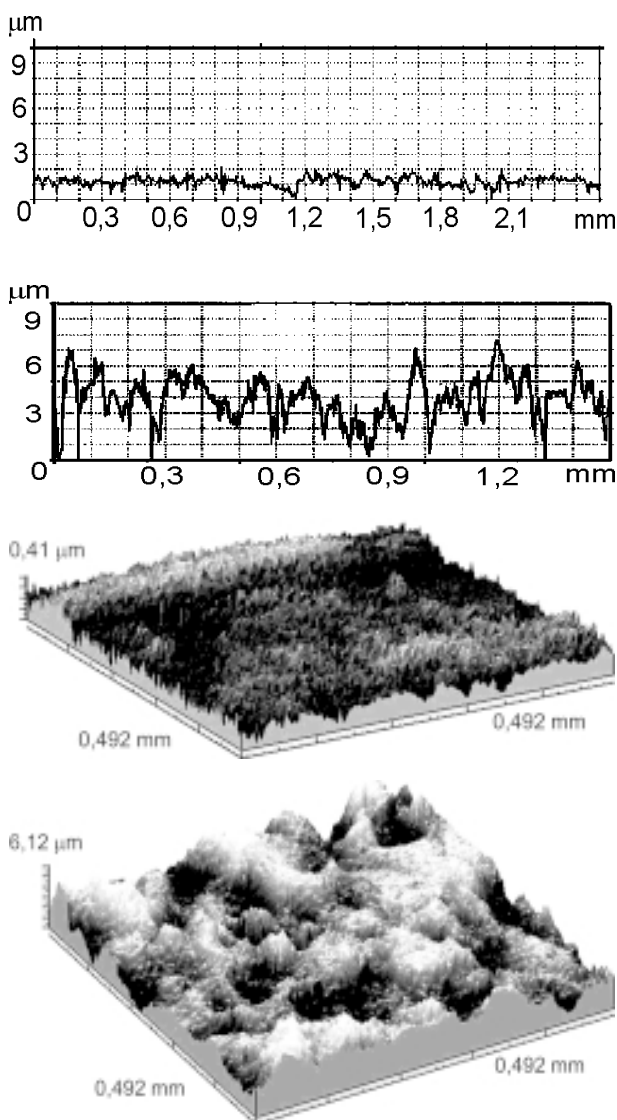


Fig. 2. Three-dimensional AFM images of the initial sample surface (1) and the deformed sample surface (2).

*Auger-spectrogram.* Fig. 3 shows Auger-spectrogram results as graphs of component depth concentration of the initial sample and of the deformed one.

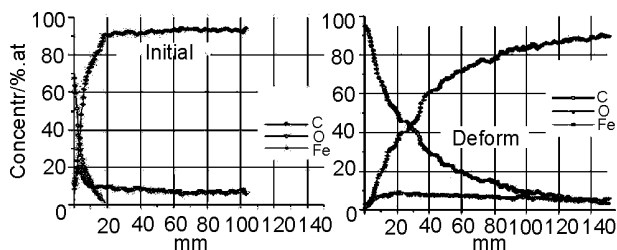


Fig. 3. AES-depth profiles of elements of samples.

The contrastive analysis of these graphs shows that after the strain cycling some radical changes took place: the levels of carbon and ferrum concentration seem to have changed over. The level of carbon concentration on the deformed sample surface corresponds to the level of ferrum concentration on the initial sample surface, and the level of ferrum concentration corresponds to the level of carbon concentration on the initial sample.

This must mean that as a result of diffusion processes carbon shifted to a more heated near-surface layer, where it could react with the alloy components – oxygen and ferrum.

Fig. 4 shows the results of the initial and the deformed samples surface scanning with a 1 mm diameter scanning beam and the scanning areas.

On the basis of the data show in fig. 4 we can conclude that:

- the carbon and the ferrum graphs are absolutely symmetrical (mirrored) which can indicate their clear chemical interaction;
- Oxygen has also become active in the deformed sample, at that the maximum peaks of the ferrum and the carbon graphs correspond to the oxygen activity spikes;
- as the scanning beam approaches the fatigue crack with the maximum deformation value, the divergence between the ferrum graph and the carbon graph increases;
- all these give us reasons to conclude that complex physical and chemical processes with the possible formation of new compounds occur in metals under cyclic loading.

Fig. 5 shows Auger-spectra of the initial and the deformed samples surfaces. Comparing these

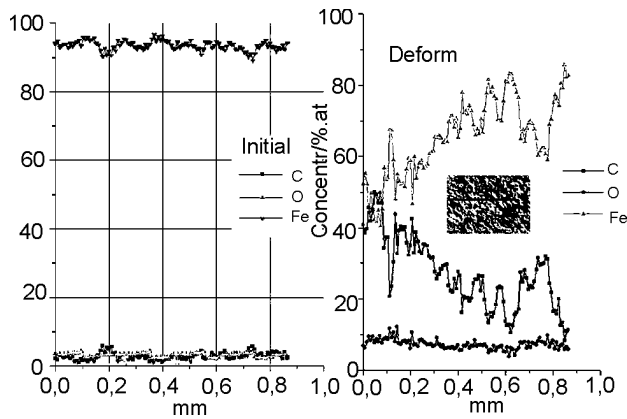


Fig. 4. AES-depth profiles of the initial sample surface (on the left) and the deformed sample surface (on the right).

spectra we can conclude that the range of carbon and oxygen Auger lines in the deformed sample has increased. That demonstrates and proves a higher content of these elements compared to the initial sample.

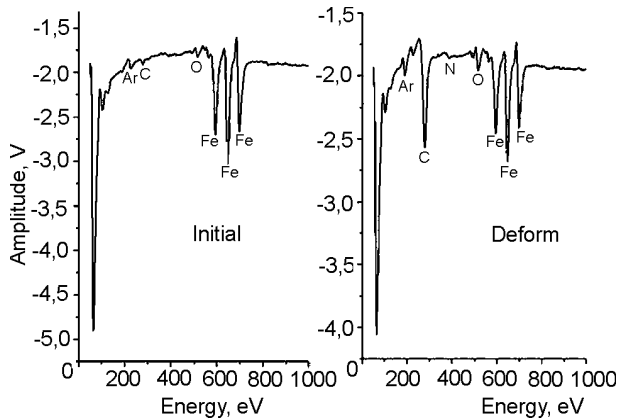


Fig. 5. Auger-spectra of the initial (on the left) and the deformed (on the right) samples surfaces.

Exact measurement of the ferrum Auger line showed that, though insignificantly, but none the less it has slightly decreased, and it shows the reduction of its concentration in the deformed sample's near-surface area.

If a part of ferrum atoms have supposedly reacted with the oxygen and carbon atoms, then such a reduction will be insignificant as the carbon content in the examined steel does not exceed 0.08 %, and the oxygen content is even less. All the more so, as fig. 1 shows, the spots are only located over an insignificant part of the deformed area.

*The results of roentgenofluorescence method examination.* One of the roentgenofluorescence method parameters is the detection of companion emission lines intensity ratio [7].

The method makes it possible to determine the form of atoms in a solid body by the ratio of integral intensity  $K_{\beta}$  of X-ray spectrum lines to integral intensity  $K_{\alpha}$ .

Fig. 6 shows measured energy spectra and calculated ratios  $Fe K_{\alpha 1,2} / Fe K_{\beta 1,2}$ .

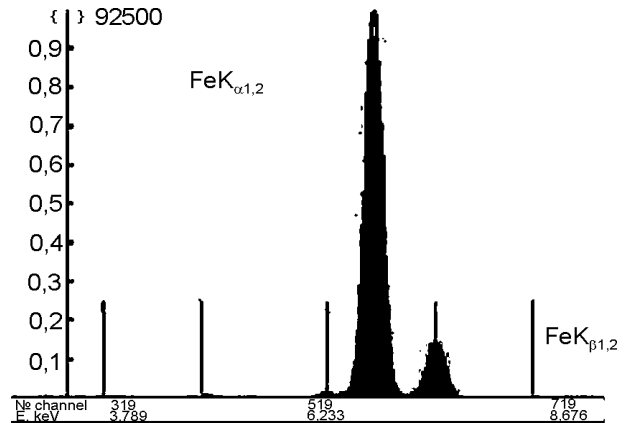


Fig. 6. Energy spectra of the deformed and the initial samples.

We got the following results: this ratio for the initial sample equals  $7.0677624 \pm 0.0005$ , and for the deformed sample it equals  $7.025773 \pm 0.0005$ . The difference between the results exceeds measuring inaccuracy and shows the change in the ferrum atoms chemical state (valency) in the deformed sample. It means that physical and chemical interaction between ferrum and the sample material components takes place under cyclic deformation. The insignificant divergence between the peaks for the deformed sample (a dashed line in fig. 6) and the initial sample is explained by the incommensurability of the ferrum content concentration and all other components – carbon and oxygen.

*X-ray diffraction analysis results.* To clarify the foregoing results we carried out an X-ray diffraction analysis of the initial and the deformed surfaces. The analysis was carried out at a diffractometer Dron-3. We analyzed three samples in different modes with chrome and cobalt- $K_{\alpha}$  emitters.

Fig. 7 shows diffractograms of the deformed sample (the upper diffractogram) and the initial sample areas.

The diffractogram analysis revealed that:

- the intensity of  $\alpha$ -Fe (200) line has decreased by the factor of 2 in the deformed areas in all three samples, and the intensity of  $\alpha$ -Fe (211)

line has increased by the factor of 1.2, which can be explained by the occurrence of texture (specific orientation of crystals);

– some weak lines appeared in the cyclically deformed surface diffractograms besides intensive  $\alpha$ -Fe lines. These lines are marked “x” in fig. 7. Their number is different in different samples, which can be explained, as the spots are located differently in each of the analyzed samples. The number of these lines depends on how many spots are in the analyzing beam focus.

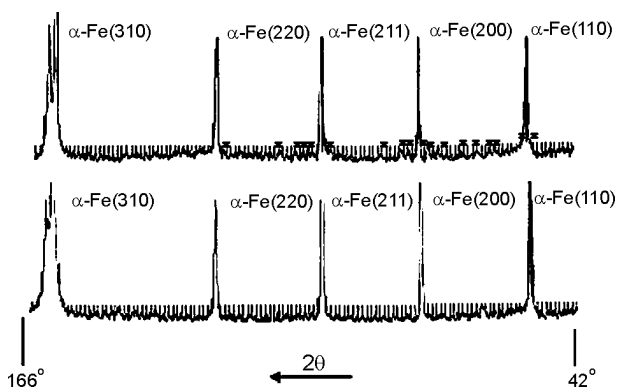


Fig. 7. X-ray diffraction pattern deformed samples (1) and the initial samples (the lower one).

The phase analysis of these lines showed that  $C_2FeO_4$  (iron oxalate) compounds are the most suitable by interplanar distances.

To clarify the results that we got at Dron-3 diffractometer, we carried out the specifying examination at X' Pert PRO PANalytical diffractometer (Holland) which confirmed the results that we had got at Dron-3 diffractometer and detected compounds  $C_2FeO_4$  (iron oxalate) and  $FeCO_3$  (iron carbonate).

To evaluate the mechanical properties of the revealed phases we measured nanohardness at NHN – S – AX – 000X nanohardness meter.

The research results showed that the revealed phases have hardness which is about twice as little as the initial grain hardness (Hv 163 and 303 correspondingly), they are probably incoherent fine-dispersed mixture of the above-mentioned compounds. When an indenter enters this phase, there appears a horizontal line in the “load – indenter depth” graph.

Pursuant to the foregoing results, new phases can occur in consequence of complex physical and chemical processes under cyclic loading.

But it is known that the formation of such compounds requires high temperature, while the

heating of the sample strained area under given conditions (loading frequency of 2800 cycles per minute) didn't exceed 1.5 °C in relation to the temperature of the environment.

The impact of the temperature on the fatigue testing results is well-known; nevertheless, thermal effects which occur in the material under the cyclic load haven't been studied enough.

The look of temperature kinetic fatigue curves depends on the crystal lattice type.

Fig. 8 shows temperature kinetic fatigue curves for different materials [8]. As it can be seen, temperature kinetic curves for face-centered cubic lattice metals mirror temperature kinetic curves for body-centered cubic lattice metals.

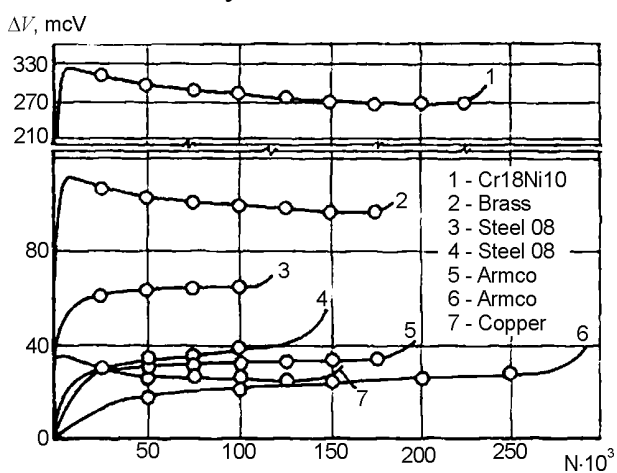


Fig. 8. Kinetic curves for different materials.

We should mention that curves which indirectly describe the fatigue process (temperature curve, internal friction curve, mechanical hysteresis loop curve, etc.) have qualitatively identical character.

The role of thermal processes at cyclic loads can be illustrated with the following example.

Fig. 9 shows the fatigue testing results of internal friction changes in steel 50 samples with and without cooling, other conditions being equal [9].

The comparative analysis of the curves shows that under normal conditions – without cooling – the kinetic curve has a look peculiar for body-centered cubic lattice metals, and with cooling it looks like a curve for face-centered cubic lattice metals. It can be assumed that this example is a convincing evidence how inner thermal processes impact the fatigue process. As for the formation of the new phases that we explore in this paper, their formation can be caused by thermal fluctuations.

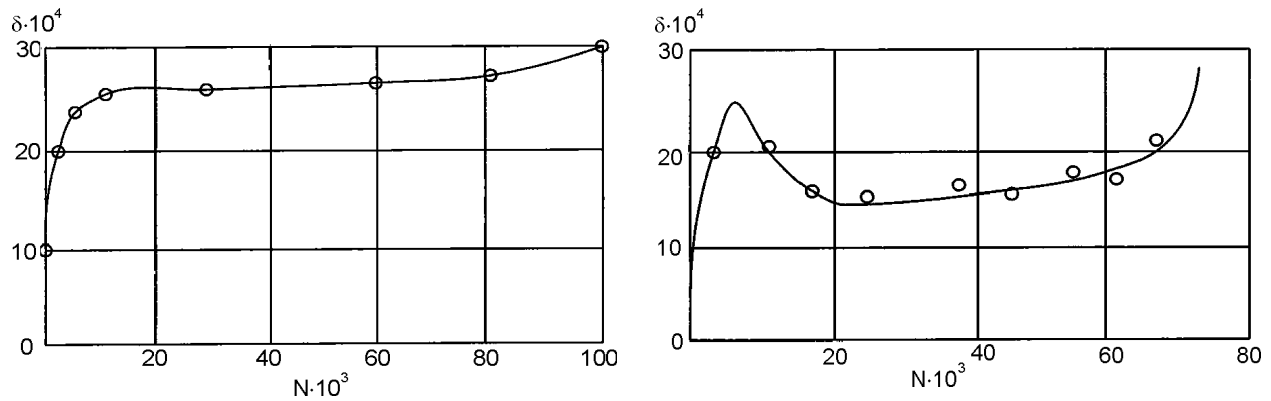


Fig. 9. Kinetic fatigue curves for steel 50 samples.

## CONCLUSION

As is evident from the foregoing, we can state that the dark spot-formations in the examined steel microstructure are new phases.

## REFERENCES

1. Panin V.E., Elsukova T.F., Panin A.V., Kuzina O.Yu., Kuznetsov P.V.//Physical Mesomechanics. – 2004. – Vol. 7, № 2. – P. 5-17.
2. Gorbachyov L.A., Lebedev T.A., Marinets T.K. On Fatigue Failure Process Periods//A Journal of Applied Mechanics and Technical Physics. – 1970. – № 5. – P. 133-136.
3. Guryev A.V., Stolyarov G.Yu. The formation of fatigue striations on a Steel Surface//The USSR Academy of Sciences Izvestiya Metals. – 1967. – № 3. – P. 133-136.
4. Gorbachyov L.A. The Research of the Temperature Fatigue Failure Kinetics//Synopsis of a Candidate of Science Thesis L. – 1971. – P. 18.
5. Lozinski M.G. The Application of High-Temperature Metallography Method in the Research of Metal and Alloy Structural Change Regularity in the Process of Their Fatigue Testing//Collection of papers: Durability of Metals under Cyclic Loading. M.: Nauka. – 1967. – p. 44-55.
6. Gorbachyov L.A., Lebedev T.A., Marinets T.K. The Research of the Temperature Fatigue Failure Kinetics//Collection of papers from Leningrad Polytechnical Institute. – 1970. – № 314. – P. 128-133.
7. Verigin A.A. Energy-Dispersive X-Ray Spectrometry Analysis and its Industrial Use. Monograph. – Tomsk: TomGU, 2005. – 241 p.
8. Gorbachyov L.A. On the Fatigue Equation for the Stationary Mode of Loading//Zavodskaya Laboratoriya. – 1972. – № 12. – P.1500-1503.
9. Kharitonov N.I., Nikolski N.N., Dronov V.S. The Research of Microflow Accumulation under Cyclic Loading// Problems of durability. – 1972. – № 9. – P. 44-48.

## ВИВЧЕННЯ СТРУКТУРИ ФІЗИКО-ХІМІЧНИХ І МЕХАНІЧНИХ ВЛАСТИВОСТЕЙ МАЛОВУГЛЕЦЕВОЇ СТАЛІ ПІСЛЯ ЦИКЛІЧНОГО НАВАНТАЖЕННЯ

Л.А. Горбачов, О.Д. Погребняк

У статті представлені результати отримані за допомогою оже-електронної спектроскопії (AES), дифракція рентгенівських променів (XRD), атомно-силової мікроскопії (AFM), рентгенофлюоресцентного аналізу, растрової і оптичної мікроскопії по дослідженню зразків СТ 3. Після циклічного навантаження показаний зв'язок між втомними характеристиками і фізико-хімічними і механічними властивостями.

## ИЗУЧЕНИЕ СТРУКТУРЫ ФИЗИКО-ХИМИЧЕСКИХ И МЕХАНИЧЕСКИХ СВОЙСТВ МАЛОУГЛЕРОДИСТОЙ СТАЛИ ПОСЛЕ ЦИКЛИЧЕСКОЙ НАГРУЗКИ

Л.А. Горбачев, А.Д. Погребняк

В статье представлены результаты полученные с помощью оже-электронной спектроскопии (AES), дифракция рентгеновских лучей (XRD), атомно-силовой микроскопии (AFM), рентгенофлюоресцентного анализа, растровой и оптической микроскопии по исследованию образцов СТ 3. После циклической нагрузки показана связь между усталостными характеристиками и физико-химическими и механическими свойствами.